Unified Representation of $\kappa-\mu$/Gamma, $\eta-\mu$/Gamma, and $\alpha-\mu$/Gamma Fading Channels Using a Mixture Gamma Distribution with Applications to Energy Detection

H. Al-Hmood, *Member, IEEE,* and H. S. Al-Raweshidy, *Senior Member, IEEE*

***Abstract*—In this letter, the performance of an energy detection (ED) is analysed over different composite generalized multipath/gamma fading channels, namely, $\kappa-\mu$/gamma, $\eta-\mu$/gamma, and $\alpha-\mu$/gamma. The mixture gamma (MG) distribution is employed to approximate with high accuracy the signal-to-noise-ratio (SNR) for all these channels. General, mathematically tractable, and unified analytic expressions for the performance metrics of ED, i.e., the average detection probability and the average area under the receiver operating characteristics curve (AUC), are derived. The validation of our analysis is verified by comparing the analytical results with the simulation results.**

***Index Terms*—Mixture gamma distribution, $\kappa-\mu$, $\eta-\mu$, $\alpha-\mu$, gamma distribution, energy detection.**

I. Introduction

THE performance of energy detection (ED) that is widely employed to perform spectrum sensing in cognitive radio (CR), has been extensively analysed over different fading channels [1]-[8]. For example, the behaviours of ED over $\kappa-\mu$ and $\eta-\mu$ fading channels, which are proposed by [9] to model the line-of-sight (LoS) and Non-line-of-sight (NLoS) communication scenarios, respectively, are studied in [5] and [8], respectively. In [4], the performance of ED over $\alpha-\mu$ fading channel, which is utilised to represent the non-homogeneous propagation environment [10], is investigated.

A part of fading channel is shadowing that may occur at the same time with the multipath fading. In the open technical literature, few works have been dedicated to study this scenario over conventional composite fading channels. In [2], the performance of ED over composite Nakagami-m/gamma fading channels, i.e., K_G is investigated by deriving the average probability of detection. Analytic expressions for the average area under the receiver operating characteristics curve (AUC) over composite Rician/gamma fading channel are given in [7]. But, these expressions are mathematically complicated and included an infinite series that is converged slowly and unsteadily. To overcome these problems, a mixture gamma (MG) distribution is suggested by [3] to approximate with high accuracy a variety of fading channels and derive unified expressions for both the average probability of detection and average AUC. However, the average probability of detection is expressed in integral form and it is applicable when the values of both the fading parameter (e.g., μ) and time-bandwidth product are integer numbers. Furthermore, the expression of the average AUC is restricted by the value of the time-bandwidth product which should be an integer number.

Motivated by the above, in this work, we firstly employ the MG distribution to represent the signal-to-noise-ratio (SNR) of the composite $\kappa-\mu$/gamma, $\eta-\mu$/gamma and $\alpha-\mu$/gamma fading channels that have not been yet studied. Then, we derive general, exact, and computationally tractable analytic expressions for both the average probability of detection and average AUC to analyse the behaviour of ED over aforementioned composite fading channels. It is noteworthy that unlike the work in [3], our derived expressions are applicable for both integer and non-integer numbers of the fading parameter and time-bandwidth product.

xxxxx xxxxx.

xxxxx xxxxx.

Manuscript received May 15, 2015.

II. Energy Detection Model

In the case of additive white Gaussian noise (AWGN), the probability of detection, $P_d(\gamma,\lambda)$, [1, eq. (5)] and probability of false alarm, $P_f(\lambda)$, [1, eq. (4)] are expressed as

$$P_d(\gamma,\lambda)=Q_u(\sqrt{2\gamma},\sqrt{\lambda}) \text{ and } P_f(\lambda)=\frac{\Gamma(u,\lambda/2)}{\Gamma(u)}. \quad (1)$$

where $\gamma=|h|^2E_s/N_0$, h, N_0, E_s and λ are the instantaneous SNR, the channel gain, the transmitted signal energy, one-side of the noise power spectral density and the pre-defined threshold value, respectively. Moreover, $\Gamma(a,b)=\int_b^\infty e^{-x}x^{a-1}dx$ is the upper incomplete gamma function [11], $\Gamma(a)=\int_0^\infty e^{-x}x^{a-1}dx$ is the gamma function [11], and $Q_u(a,b)=\int_b^\infty \frac{x^u}{a^{u-1}}e^{-\frac{x^2+a^2}{2}}I_{u-1}(ax)dx$ is the generalized Marcum-Q function [6] where u and $I_a(.)$ represent the time-bandwidth product and the modified Bessel function of the first kind and ath order, respectively.[1].

III. The MG Distribution for Composite $\kappa-\mu$/gamma, $\eta-\mu$/gamma and $\alpha-\mu$/gamma Fading Channels

The probability density function (PDF) of the instantaneous SNR, γ, ($f_\gamma(\gamma)$) of wireless fading channel can be expressed by the MG distribution as [3, eq. (1)]

$$f_\gamma(\gamma)=\sum_{i=1}^{N}\tilde{\alpha}_i\gamma^{\beta_i-1}e^{-\zeta_i\gamma}. \quad (2)$$

[1]It can be noted that $u=S/2$ and $1+u=S/2$where S is the number of samples [1].

where N is the number of terms and $\tilde{\alpha}_i$, β_i and ζ_i are the parameters of ith Gamma component. It can be observed that the main problem in using the MG is how to determine N. In [3], some methods are proposed to compute a minimum N that achieves good approximation with high accuracy. One of these methods is based on evaluating the mean square error (MSE) between the PDF of the exact distribution and the PDF of the approximate distribution that is modelled by the MG distribution.

In the remainder of this section, the parameters of the MG distribution for different composite channels are derived as:

A. $\kappa-\mu$/gamma Fading Channel

The $\kappa-\mu$ contains two parameters which are κ and μ. The former represents the ratio between the total power of the dominant components and the scattered waves whereas the latter, which is also presented in the $\eta-\mu$ and $\alpha-\mu$, represents the real extension of the number of the multipath clusters. The $\kappa-\mu$/gamma fading channel is a composite fading channel from the $\kappa-\mu$ fading channel and gamma distribution which models the shadowing. Accordingly, the SNR distribution of the $\kappa-\mu$/gamma fading channel can be evaluated by averaging [9, eq. (10)] over gamma distribution [2, eq. (4)] as follows

$$f_\gamma(\gamma) = \frac{\mu(1+\kappa)^{\frac{\mu+1}{2}}\gamma^{\frac{\mu-1}{2}}}{\Gamma(k)\Omega^k\kappa^{\frac{\mu-1}{2}}e^{\mu\kappa}} \times\int_0^\infty y^{k-\frac{\mu}{2}-\frac{3}{2}}e^{-\frac{\mu(1+\kappa)\gamma}{y}-\frac{y}{\Omega}}I_{\mu-1}\left(2\mu\sqrt{\frac{\mu(1+\kappa)\gamma}{y}}\right)dy. \quad (3)$$

where k is the shaping parameter and Ω is the mean power.

By substituting $x=\frac{\mu(1+\kappa)\gamma}{y}$ in (3), this yields

$$f_\gamma(\gamma) = \vartheta_{\kappa-\mu}\gamma^{k-1}\int_0^\infty e^{-x}g(x)dx. \quad (4)$$

where $\vartheta_{\kappa-\mu} = -\frac{\mu^{k-\frac{\mu-1}{2}}}{\Gamma(k)\kappa^{\frac{\mu-1}{2}}e^{\mu\kappa}}\left(\frac{1+\kappa}{\Omega}\right)^k$ and $g(x) = x^{\frac{\mu}{2}-k-\frac{1}{2}}e^{-\frac{\mu(1+\kappa)\gamma}{\Omega x}}I_{\mu-1}\left(2\mu\sqrt{x}\right)$. The integration in (4), $\mathcal{S}=\int_0^\infty e^{-x}g(x)dx$, can be approximated as a Gaussian-Laguerre quadrature sum as $\mathcal{S}\approx\sum_{i=1}^N w_i g(x_i)$ where x_i and w_i are the abscissas and weight factors for the Gaussian-Laguerre integration, respectively [12]. Consequently, (4) can be expressed by the MG distribution with parameters

$$\tilde{\alpha}_i = \frac{\theta_i}{\sum_{l=1}^N\theta_l\Gamma(\beta_l){\zeta_l}^{-\beta_l}}, \quad \beta_i=k, \quad \zeta_i=\frac{\mu(1+\kappa)}{\Omega x_i}, \quad \theta_i=\vartheta_{\kappa-\mu}w_i x_i^{\frac{\mu}{2}-k-\frac{1}{2}}I_{\mu-1}\left(2\mu\sqrt{x_i}\right). \quad (5)$$

B. $\eta-\mu$/gamma Fading Channel

The $\eta-\mu$ includes two parameters which are η and μ. The definition of η depends on the type of format. In format 1, η represents the power ratio between the in-phase and quadrature scattered components in each multipath cluster with $0<\eta<\infty$. The respective H and h are expressed by $H=(\eta^{-1}-\eta)/4$ and $h=(2+\eta^{-1}+\eta)/4$, respectively. In format 2, η stands for the correlation coefficient between the in-phase and quadrature scattered components in each multipath cluster with $-1<\eta<1$. The respective H and h are given by $H=\eta/(1-\eta^2)$ and $h=1/(1-\eta^2)$, respectively [9].

The SNR distribution of the $\eta-\mu$/gamma fading channel can be found by integrating the $\eta-\mu$ fading channel [9, eq. (26)] over [2, eq. (4)] as follows

$$f_\gamma(\gamma) = \frac{2\sqrt{\pi}h^\mu\mu^{\mu+\frac{1}{2}}\gamma^{\mu-\frac{1}{2}}}{\Gamma(\mu)\Gamma(k)\Omega^k H^{\mu-\frac{1}{2}}} \times\int_0^\infty y^{k-\mu-\frac{3}{2}}e^{-\frac{2\mu h\gamma}{y}-\frac{y}{\Omega}}I_{\mu-\frac{1}{2}}\left(\frac{2\mu H\gamma}{y}\right)dy. \quad (6)$$

By assuming $x=\frac{2\mu h\gamma}{y}$ and following the same procedure for the $\kappa-\mu$/gamma fading channel, we obtain

$$\tilde{\alpha}_i = \frac{\theta_i}{\sum_{l=1}^N\theta_l\Gamma(\beta_l){\zeta_l}^{-\beta_l}}, \quad \beta_i=k, \quad \zeta_i=\frac{2\mu h}{\Omega x_i}, \quad \theta_i=\vartheta_{\eta-\mu}w_i x_i^{\mu-k-\frac{1}{2}}I_{\mu-\frac{1}{2}}\left(\frac{H}{h}x_i\right). \quad (7)$$

where $\vartheta_{\eta-\mu} = -\frac{\sqrt{\pi}2^{k-\mu+\frac{1}{2}}h^{k-\frac{1}{2}}}{\Gamma(\mu)\Gamma(k)H^{\mu-\frac{1}{2}}}\left(\frac{\mu}{\Omega}\right)^k$.

C. $\alpha-\mu$/gamma Fading Channel

The $\alpha-\mu$ distribution is used to model the non-linear environment of wireless communications. Due to a limited space, please refer to [10] for further information.

The SNR distribution of composite $\alpha-\mu$/gamma can be computed by using [10, eq. (1)] and [2, eq. (4)] as follows

$$f_\gamma(\gamma) = \frac{\alpha\mu^\mu\gamma^{\frac{\alpha\mu}{2}-1}}{2\Gamma(\mu)\Gamma(k)\Omega^k}\int_0^\infty y^{k-\frac{\alpha\mu}{2}-1}e^{-\frac{\mu\gamma^{\alpha/2}}{y^{\alpha/2}}-\frac{y}{\Omega}}dy. \quad (8)$$

where $\alpha>0$ is the non-linear fading parameter.

By using $x=\frac{\mu\gamma^{\alpha/2}}{y^{\alpha/2}}$ and following a similar procedure for the $\kappa-\mu$/gamma channel, the parameters of MG distribution for the $\alpha-\mu$/gamma fading channel are obtained as

$$\tilde{\alpha}_i = \frac{\theta_i}{\sum_{l=1}^N\theta_l\Gamma(\beta_l){\zeta_l}^{-\beta_l}}, \quad \beta_i=k, \quad \zeta_i=\frac{\mu^{2/\alpha}}{\Omega x_i^{2/\alpha}}, \quad \theta_i=\vartheta_{\alpha-\mu}w_i x_i^{\mu-\frac{2k}{\alpha}-1}. \quad (9)$$

where $\vartheta_{\alpha-\mu} = -\frac{\mu^{2k/\alpha}}{\Gamma(\mu)\Gamma(k)\Omega^k}$.

IV. Average Probability of Detection

The average probability of detection, $\overline{P_d}(\lambda)$, can be evaluated by [8, eq. (4)]

$$\overline{P_d}(\lambda) = \int_0^\infty P_d(\gamma,\lambda)f_\gamma(\gamma)d\gamma. \quad (10)$$

When $u\in\mathbb{R}$, i.e., u is a real number, the $\overline{P_d}(\lambda)$ can be found as [see Appendix A]

$$\overline{P_d}(\lambda) = 1-\frac{2^{-u}\lambda^u e^{-\frac{\lambda}{2}}}{\Gamma(1+u)}\sum_{i=1}^N\frac{\tilde{\alpha}_i\Gamma(\beta_i)}{(1+\zeta_i)^{\beta_i}} \times\Phi_2\left(\beta_i,1;1+u;\frac{\lambda}{2},\frac{\lambda}{2(1+\zeta_i)}\right). \quad (11)$$

where $\Phi_2(.)$ is the bivariate confluent hypergeometric function defined in [11, eq. (9.261.2)].

It can be noted that $\Phi_2(.)$ is not yet implemented in common mathematical packages such as MATLAB and MATHEMATICA software. Therefore, a series convergence is assumed by a limited number of terms, R, with truncation error, E_R.

By invoking [11, eq. (9.261.2)] and using the identity $(a)_{b+c} = (a)_b(a+b)_c$, E_R for (11) can be expressed as

$$E_R = \sum_{i=1}^{N} \frac{\tilde{\alpha}_i \Gamma(\beta_i)}{(1+\zeta_i)^{\beta_i}} \sum_{n=0}^{\infty} \frac{(1)_n}{(1+u)_n n!} \left(\frac{\lambda}{2}\right)^n \times {}_1F_1\left(\beta_i; 1+u+n; \frac{\lambda}{2(1+\zeta_i)}\right). \quad (12)$$

where $(.)_R$ and ${}_1F_1(.)$ are the Pochhammer symbol and the confluent hypergeometric function, respectively.

It can be observed that ${}_1F_1(.)$ in (12) is monotonically decreasing with n. Accordingly, after following the same procedure in [13], this yields

$$E_R \leq \frac{(1)_R(\frac{\lambda}{2})^R}{(1+u)_R R!} \sum_{i=1}^{N} \frac{\tilde{\alpha}_i \Gamma(\beta_i)}{(1+\zeta_i)^{\beta_i}} {}_1F_1\left(1; 1+u+R; \frac{\lambda}{2}\right) \times {}_1F_1\left(\beta_i; 1+u+R; \frac{\lambda}{2(1+\zeta_i)}\right). \quad (13)$$

The tightness of the upper bound of (11) for all composite fading channels is verified here by numerically evaluating the integration in (10) using the trapezoidal integration routine in MATLAB software. Then the results are compared with their analytical and simulation counterparts as shown in Table I. It can be noted from this table that the difference between the provided results is approximately zero.

When u is an integer number, i.e., $u \in \mathbb{Z}$, the $\overline{P_d}(\lambda)$ can be computed by substituting $P_d(\gamma, \lambda)$ of (1) and (2) into (10) with the help of [14, eq. (9)] and [11, eq. (3.35.3)]. Consequently, after some mathematical operations, this yields

$$\overline{P_d}(\lambda) = \frac{e^{-\frac{\lambda}{2}}}{\Gamma(2-u)} \sum_{i=1}^{N} \frac{\tilde{\alpha}_i \Gamma(\beta_i - u + 1)}{(1+\zeta_i)^{\beta_i - u + 1}} \times \Phi_1\left(\beta_i - u + 1, 1; 2-u; \frac{1}{1+\zeta_i}, \frac{\lambda}{2(1+\zeta_i)}\right). \quad (14)$$

where $\Phi_1(.)$ is another form of the bivariate confluent hypergeometric function defined in [11, eq. (9.261.1)][2]. This function is also not available in MATLAB and MATHEMATICA software packages. Therefore, a series convergence is assumed.

Using [11, eq. (9.261.1)] and following the same methodology in (12), E_R for (14) can be obtained as

$$E_R \leq \frac{(\beta_i - u)_R (1)_R}{(2-u)_R R!} \sum_{i=1}^{N} \frac{\tilde{\alpha}_i \Gamma(\beta_i - u + 1)}{(1+\zeta_i)^{\beta_i - u + 1}} \left(\frac{1}{1+\zeta_i}\right)^R \times {}_2F_1\left(\beta_i - u + R, 1; 2-u+R; \frac{1}{1+\zeta_i}\right) \times {}_1F_1\left(\beta_i - u + R; 2-u+R; \frac{\lambda}{2(1+\zeta_i)}\right). \quad (15)$$

where ${}_2F_1(.)$ is the Gaussian hypergeometric function.

[2]The function $\Phi_1(.)$ can be evaluated by its Euler-type representation and standard numerical integration methods [15, eq. (8)].

TABLE I
COMPARISON OF NUMERICAL INTEGRATION, ANALYTICAL, AND SIMULATION VALUES OF $\overline{P_d}(\lambda)$ OVER DIFFERENT COMPOSITE CHANNELS WITH $\mu = 0.5$, $k = 4.5$, $\bar{\gamma} = 15$ *dB*, $N = 15$, $u = 1.5$, AND $E_R \leq 10^{-7}$.

Channel	$\overline{P_d}(\lambda)$ Integration	$\overline{P_d}(\lambda)$ Analytical	$\overline{P_d}(\lambda)$ Simulation
$\kappa - \mu$, $\kappa = 2.5$	0.764712	0.765723	0.763800
$\eta - \mu$, $\eta = 0.7$	0.904627	0.905435	0.904717
$\alpha - \mu$, $\alpha = 3$	0.973688	0.965964	0.973789

V. AVERAGE AREA UNDER THE ROC CURVE

The average AUC, $\bar{A}$, is given as [7, eq. (33)]

$$\bar{A} = \frac{1}{2^u \Gamma(u)} \int_0^{\infty} \lambda^{u-1} e^{-\frac{\lambda}{2}} \overline{P_d}(\lambda) d\lambda. \quad (16)$$

Substituting (11) into (16) with the aid of [11, eq. (9.261.2)], [11, eq. (3.35.3)] and $\Gamma(a+b) = (a)_b \Gamma(a)$, $\bar{A}$ for $u \in \mathbb{R}$ can be found as

$$\bar{A} = 1 - \frac{\Gamma(2u)}{u[2^u \Gamma(u)]^2} \sum_{i=1}^{N} \frac{\tilde{\alpha}_i \Gamma(\beta_i)}{(1+\zeta_i)^{\beta_i}} \times F_1\left(2u, 1, \beta_i; 1+u; \frac{1}{2}, \frac{1}{2(1+\zeta_i)}\right). \quad (17)$$

where $F_1(.)$ is the double variables Appell hypergeometric function [11, eq. (9.180.1)] and its a standard built-in function available in MATHEMATICA software package.

When $u \in \mathbb{Z}$, $\bar{A}$ can be expressed as

$$\bar{A} = \frac{1}{2^u \Gamma(2-u)} \sum_{i=1}^{N} \frac{\tilde{\alpha}_i \Gamma(\beta_i - u + 1)}{(1+\zeta_i)^{\beta_i - u + 1}} \times F_1\left(\beta_i - u + 1, 1, u; 2-u; \frac{1}{1+\zeta_i}, \frac{1}{2(1+\zeta_i)}\right). \quad (18)$$

The expression in (18) is evaluated by using (14) and (16) with the help of [11, eq. (9.261.1)] and [11, eq. (3.35.3)] and doing some mathematical simplifications.

VI. ANALYTICAL AND SIMULATION RESULTS

In this section, Monte Carlo simulations with 10^6 iterations are utilized to compare the simulation results with the analytical results of ED over $\kappa-\mu$/gamma, $\eta-\mu$/gamma (format 1), and $\alpha-\mu$/gamma fading channels. In all figures, the numerical results are represented by solid lines with marks while the simulated results are shown by dot marks. To achieve MSE $\leq 10^{-6}$ between the exact PDF and approximate PDF using a MG distribution, N is selected as 15 for all channels.

Fig. 1 and Fig. 2 show the complementary receiver operating characteristics curve (CROC) which plots the average probability of missed-detection, $\overline{P_{md}}(\lambda)$, ($\overline{P_{md}}(\lambda) = 1 - \overline{P_d}(\lambda)$) versus $P_f(\lambda)$ and the complementary AUC (1-$\bar{A}$) versus average SNR, respectively. In both figures, the simulation parameters are κ = 2.5, η = 0.7, α = 3, k = 4.5, $\bar{\gamma}$ = 15 dB, and u = 1.5. Moreover, numbers of terms, R, in Fig. 1 that are required to evaluate (12) at P_f = 0.1 with seven figure accuracy for $\alpha-\mu$/gamma, $\eta-\mu$/gamma and $\kappa-\mu$/gamma are 20, 21, and 22, respectively. From the provided figures, it is

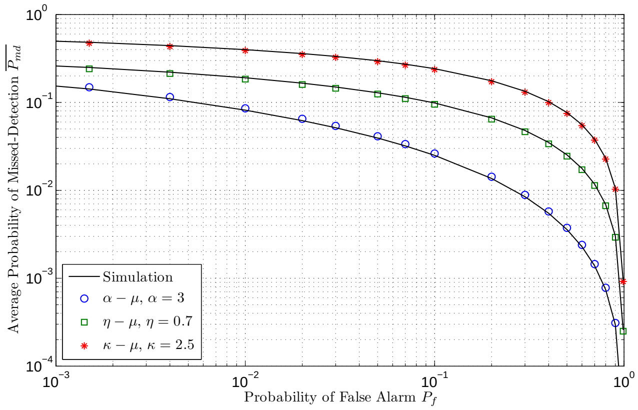

Fig. 1. Complementary ROC curves over $\kappa-\mu$/gamma, $\eta-\mu$/gamma and $\alpha-\mu$/gamma fading channels for μ = 0.5, k = 4.5, $\bar{\gamma}$ = 15 dB and u = 1.5.

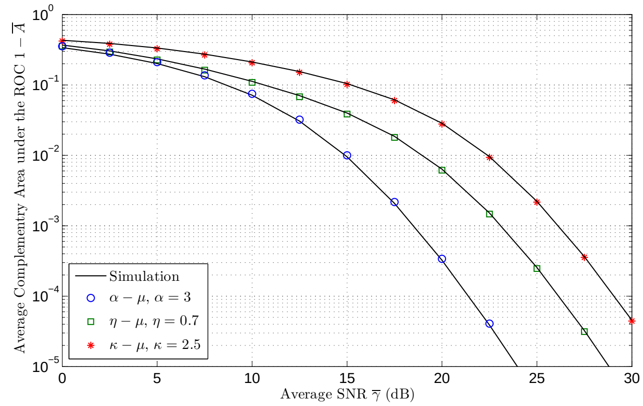

Fig. 2. Complementary AUC curves versus $\bar{\gamma}$ over $\kappa-\mu$/gamma, $\eta-\mu$/gamma and $\alpha-\mu$/gamma fading channels for μ = 0.5, k = 4.5 and u = 1.5.

clear that the numerical results match well with their Monte Carlo simulation counterparts, proving the high accuracy of the analysis using a MG distribution.

It can be observed that the results in Fig. 1 and Fig. 2 can not be obtained by [3, eq. (29)] and [3, eq. (33)], respectively. This is because [3, eq. (29)] is valid when the values of β_i (i.e., k) and u are integer and [3, eq. (33)] is applicable for integer-valued of u.

VII. Conclusions

In this letter, the performance of ED over composite $\kappa-\mu$/gamma, $\eta-\mu$/gamma and $\alpha-\mu$/gamma fading channels was analysed by using a MG distribution. Novel, general, unified, and not limited analytic expressions for both the average probability of detection and average AUC were derived. The provided numerical results using a MG distribution were matched exceedingly with the Monte Carlo simulation results. The behaviour of ED over $\kappa-\mu$, $\eta-\mu$ and $\alpha-\mu$ fading channels can be studied by inserting $k\rightarrow\infty$ in our derived expressions. Furthermore, the results of this paper can be employed to analyse the performance of ED over different composite fading channels such as Nakagami-m/gamma.

Appendix A
Proof of (11)

When $u\in\mathbb{R}$, the $P_d(\gamma,\lambda)$ of (1) can be expressed by [14, eq. (34)] as follows

$$P_d(\gamma,\lambda)=1-\left(\frac{\lambda}{2}\right)^u e^{-\frac{2\gamma+\lambda}{2}}\tilde{\Phi}_3\Big(1;1+u;\frac{\lambda}{2},\frac{\gamma\lambda}{2}\Big). \quad (19)$$

where $\tilde{\Phi}_3(.)$ is the regularized bivariate confluent hypergeometric function defined in [14, eq. (4)].

Inserting (2) and (19) into (10) with the help of [14, eq. (4)] and $\int_0^\infty f_\gamma(\gamma)d\gamma\triangleq 1$, this yields

$$\overline{P_d}(\lambda)=1-\frac{\lambda^u e^{-\frac{\lambda}{2}}}{2^u\Gamma(1+u)}\sum_{i=1}^{N}\tilde{\alpha}_i\sum_{l=0}^{\infty}\sum_{m=0}^{\infty}\frac{(1)_l}{(1+u)_{l+m}l!m!}\left(\frac{\lambda}{2}\right)^l\left(\frac{\lambda}{2}\right)^m\int_0^\infty\gamma^{m+\beta_i-1}e^{-(1+\zeta_i)\gamma}d\gamma. \quad (20)$$

Using [11, eq. (3.35.3)] to evaluate the integration in (20) and invoking the identity $\Gamma(a+b)=(a)_b\Gamma(a)$, the desired result in (11) is deduced.

References

[1] F. F. Digham, M. S. Alouini, and M. K. Simon, “On the energy detection of unknown signals over fading channels,” *IEEE Trans. Commun.*, vol. 55, no. 1, pp. 21-24, Jan. 2007.

[2] S. Atapattu, C. Tellambura, and H. Jiang, “Performance of an energy detector over channels with both multipath fading and shadowing,” *IEEE Trans. Wireless Commun.*, vol. 9, no. 12, pp. 3662-3670, Dec. 2010.

[3] S. Atapattu, C. Tellambura, and H. Jiang, “A mixture gamma distribution to model the SNR of wireless channels,” *IEEE Trans. Wireless Commun.*, vol. 10, no. 12, pp. 4193-4203, Dec. 2011.

[4] Y. Fathi, and M. H. Tawfik “Versatile performance expression for energy detector over $\alpha-\mu$ generalised fading channels,” *Elect. Lett.*, vol. 48, no. 17, pp. 1081-1082, Aug. 2012.

[5] P. C. Sofotasios et al., “Energy detection based spectrum sensing over $\kappa-\mu$ and $\kappa-\mu$ extreme fading channels,” *IEEE Trans. Veh. Technol.*, vol. 62, no. 3, pp. 1031-1040, Mar. 2013.

[6] P. C. Sofotasios, L. Mohjazi, S. Muhaidat, M. Al-Qutayri, and G. K. Karagiannidis, “Energy detection of unknown signals over cascaded fading channels,” *IEEE Antennas Wireless Propag. Lett.*, vol. PP, no. 99, pp.1-1, 2015.

[7] K. P. Peppas, G. Efthymoglou, V. A. Aalo, M. Alwakeel, and S. Alwakeel, “Energy detection of unknown signals in Gamma-shadowed Rician fading environments with diversity reception,” *IET Commun.*, vol. 9, no. 2, pp. 196-210, Jan. 2015.

[8] H. Al-Hmood, and H. S. Al-Raweshidy, “Performance analysis of energy detector over $\eta-\mu$ fading channel: PDF-based approach,” *Elect. Lett.*, vol. 51, no. 3, pp. 249-251, Feb. 2015.

[9] M. D. Yacoub, “The $\kappa-\mu$ distribution and the $\eta-\mu$ distribution,” *IEEE Antennas Propag. Mag.*, vol. 49, no. 1, pp. 68-81, Feb. 2007.

[10] M. D. Yacoub, “The $\alpha-\mu$ distribution: a physical fading model for the Stacy distribution,” *IEEE Trans. Veh. Technol.*, vol. 56, no. 1, pp. 27-34, Jan. 2007.

[11] I. S. Gradshteyn and I. M. Ryzhik, *Table of Integrals, Series and Products*, 7th edition. Academic Press Inc., 2007.

[12] M. Abramowitz and I. A. Stegun, editors, *Handbook of Mathematical Functions: With Formulas, Graphs, and Mathematical Tables.* Dover Publications, 1965.

[13] C. C. Tan, and N. C. Beaulieu, “Infinite series representation of the bivariate Rayleigh and Nakagami-m distributions,” *IEEE Trans. Commun.*, vol. 45, no. 10, pp. 1159-1161, Oct. 1997.

[14] D. Morales-Jimenez, F. J. Lopez-Martinez, E. Martos-Naya, J. F. Paris, and A. Lozano, “Connections between the generalized Marcum-Q function and a class of hypergeometric functions,” *IEEE Trans. Inf. Theory*, vol. 60, no. 2, pp. 1077-1082, Feb. 2014.

[15] F. J. Lopez-Martinez, R. F. Pawula, E. Martos-Naya, and J. F. Paris, “A clarification of the proper-integral form for the Gaussian Q-function and some new results involving the F-function,” *IEEE Commun. Lett.*, vol. 18, no. 9, pp. 1495-1498, Sept. 2014.